Progress In Electromagnetics Research C, Vol. 173, 92–102, 2026

PIER C

(Received 24 April 2026, Accepted 17 June 2026, Scheduled 2 September 2026)

High-Gain Ultra-Wideband Half-Moon Monopole Patch Antenna with a Metallic Reflector for Ground-Penetrating Radar (GPR) Systems

M. I. H. K. Anuar[1], A. Gupta[2,7], A. D. Khaleel[3], Z. Zakaria[1], N. Nurhayati[4], A. A. G. Amer[5], F. H. Partiansyah[6,*], H. Omar[7], A. Varshney[8], R. George[7], A. M. Kassim[9,*], and A. J. A. Al-Gburi[7,*]

[1]*Center for Telecommunication Research & Innovation (CeTRI)*
Fakulti Teknologi Dan Kejuruteraan Elektronik Dan Komputer (FTKEK), Universiti Teknikal Malaysia Melaka (UTeM)
Jalan Hang Tuah Jaya, 76100, Durian Tunggal, Melaka, Malaysia
[2]*Department of Electronics and Communication Engineering, Chandigarh University, Punjab, India*
[3]*Computer Engineering Department, College of Engineering, Al-Iraqia University, Iraq*
[4]*Department of Electrical Engineering, Universitas Negeri Surabaya, Surabaya 60231, Indonesia*
[5]*Institute for Mathematical Research (INSPEM), Universiti Putra Malaysia (UPM), Serdang, Selangor 43400, Malaysia*
[6]*Department of Electrical Engineering, Universitas Brawijaya, Malang, Indonesia*
[7]*Strategic Research Institute (SRI), Asia Pacific University, Jalan Teknologi 5, Taman Teknologi Malaysia*
Kuala Lumpur 57000, Malaysia
[8]*ECE Department, Graphic Era (Deemed to be University), Dehradun-248002, India*
[9]*Center of Robotics and Industrial Automation, Faculty of Technology and Electrical Engineering*
Universiti Teknikal Malaysia Melaka, Hang Tuah Jaya, 76100 Durian Tunggal, Melaka, Malaysia

ABSTRACT: In this study, a coplanar waveguide (CPW)-fed half-moon monopole ultra-wideband (UWB) antenna is proposed, simulated, fabricated, and experimentally validated for ground-penetrating radar (GPR) applications. The antenna is specially designed to provide high forward gain and stable wideband performance via integrating a full-copper metallic reflector. The proposed antenna exhibits good impedance matching and satisfactory reflection coefficient characteristics across the UWB frequency range of 3.1–10.6 GHz. By incorporating the metallic reflector, a significant radiation enhancement is achieved. The antenna attains a peak gain of 8.7 dBi at 6 GHz and maintains a gain above 6.5 dBi throughout the operating bandwidth. This gain improvement and suppression of back radiation are particularly important for GPR systems, where deep subsurface penetration and high-resolution imaging are essential. The integration of a metallic reflector provides a simple yet highly effective approach for gain enhancement without complex structures or advanced materials, as confirmed by both simulated and experimental results. These findings demonstrate the suitability of the proposed antenna for practical high-gain UWB GPR and broadband sensing applications.

1. INTRODUCTION

Ultra-wideband (UWB) antenna technology has become one of the most active research areas in wireless communications due to its wide bandwidth, compact size, and suitability for applications such as ground-penetrating radar (GPR), medical imaging, and high-data-rate communication systems. In GPR applications, antennas are required to maintain a wide impedance bandwidth while providing high gain and stable radiation characteristics to ensure sufficient penetration depth and high-resolution imaging. Consequently, extensive research has been conducted on printed monopole and microstrip patch antennas for UWB applications, as these antennas offer compact, low-profile solutions that are particularly well suited for portable and field-deployable systems [1–6].

Metallic reflectors have attracted significant attention in the antenna community due to their simple structure, low fabrication cost, ease of implementation, and ability to provide consistent gain enhancement across a wide frequency range. Unlike frequency-selective surfaces (FSSs) and metasurface reflectors, which often require complex unit-cell designs and precise fabrication processes, conventional metallic reflectors offer a practical and cost-effective solution for improving antenna directivity and radiation performance [7]. Therefore, metallic reflectors remain an attractive choice for wireless communication, radar, and sensing applications, where broadband operation, mechanical robustness, and low-cost implementation are desired. Recent studies have demonstrated that metallic reflectors can achieve competitive gain enhancement while maintaining design simplicity and fabrication accessibility [8, 9].

In recent years, various approaches have been explored to improve the gain and bandwidth performance of UWB antennas. These approaches include microstrip arrays, modified monopole geometries, parasitic elements, and aperture-based structures. For example, Jayamani et al. introduced UWB microstrip patch antennas specifically designed for biomedical

* Corresponding authors: Ahmed Jamal Abdullah Al-Gburi (ahmedjamal@ieee.org); Anuar Mohamed Kassim (anuar@utem.edu.my); Fakhriy Hario Partiansyah (fakhriy08@ub.ac.id).

monitoring applications [10]. Similarly, Kalita et al. optimized UWB patch antennas for GPR applications, demonstrating enhanced penetration capabilities across the UWB frequency range [11]. In addition, metasurface-inspired and reflector-backed antenna designs have been widely investigated because of their ability to significantly improve antenna gain and radiation directivity [12–15]. However, many of these approaches increase fabrication complexity, alignment requirements, and implementation costs.

In GPR systems, gain enhancement remains an important design challenge. Conventional UWB monopole antennas typically exhibit omnidirectional radiation patterns, resulting in relatively low forward gain and reduced subsurface imaging performance. To address this limitation, several studies have investigated reflector-backed UWB antennas to improve gain, directivity, and penetration efficiency [16–18]. Representative examples for GPR applications can be found in [19–23], while similar concepts have also been successfully applied to medical imaging systems [24–28], where compact and high-gain antenna configurations are highly desirable. Nevertheless, there remains need for simple, low-cost, and easily fabricated solutions capable of enhancing gain while preserving inherent wideband characteristics of CPW-fed monopole antennas.

Although several UWB antennas have been reported for GPR applications, many existing designs rely on complex antenna geometries, large physical dimensions, antenna arrays, or additional structures such as frequency-selective surfaces (FSSs), electromagnetic bandgap (EBG) structures, and metasurfaces to achieve high gain and directional radiation characteristics. These approaches often increase fabrication complexity, cost, and overall antenna size, limiting their suitability for compact and low-cost GPR systems. To address these limitations, the proposed antenna employs a simple half-moon monopole geometry integrated with a metallic reflector to enhance gain and directivity while maintaining a compact structure and wide impedance bandwidth. The design offers an attractive balance between performance, simplicity, and fabrication cost, making it a promising candidate for portable and real-world GPR applications. Simulation and experimental analyses verify good impedance matching in the UWB frequency range, with a peak gain of up to 8.7 dBi. By incorporating a full-copper reflector, the proposed antenna not only improves radiation directivity but also enhances subsurface signal penetration, making it highly suitable for practical GPR applications. These results highlight the potential of the proposed design as a compact, high-gain, cost-effective solution for next-generation GPR and broadband sensing systems.

2. DESIGN OF UWB CPW-FED HALFMOON MONOPOLE PATCH ANTENNA

The designed antenna is fabricated on an FR-4 substrate with a relative permittivity of 4.3, a substrate thickness of 1.6 mm, and the antenna's dimensions are as large as $70 \times 70\,\text{mm}^2$, including the feeding structure [5]. This design uses a coplanar waveguide (CPW) feeding technique which offers broad impedance bandwidth, very good single-layer metallization quality, and easy integration with active circuitry. The design targets conventional UWB monopole antenna characteristics, such as moderate gain and compromised performance at lower frequencies of the UWB spectrum, which restrict its applications in ground-penetrating radar (GPR), biomedical sensing, and high-data-rate wireless link. A half-moon-shaped radiator with geometrical modifications is presented, and its performance improvement is highlighted by adding a full copper reflector. Fig. 1 illustrates the radiating element of the proposed antenna, which consists of an elliptical half-moon patch, a circular stub, and a triangular stub. The elliptical section, defined by the horizontal radius (R) and vertical radius ($R1$), primarily determines the antenna's fundamental resonant modes. A circular stub with radius ($R2$) is attached laterally to increase the effective surface current path, thereby enhancing impedance bandwidth. In addition, a triangular stub with height (Tl) is embedded at the top of the radiating patch to provide capacitive loading and improve impedance matching, particularly at higher frequencies. The combination of the elliptical half-moon patch, circular stub, and triangular stub creates a hybrid radiating structure capable of generating multiple resonant modes, thereby supporting ultra-wideband operation. The proposed antenna, both with and without the metallic reflector, is presented in Fig. 1.

A CPW feedline with specified width (Wf) and length (Lf), which is matched to a characteristic impedance of $50\,\Omega$, excites the antenna. There is a gap of (Gw) between the feedline and ground planes. They are also additionally symmetrically truncated from below, along with ground planes of dimensions $W1$, $W2$, Lg, $Lg1$, and $Lg2$, which adjust impedance bandwidth and make radiation patterns stable. These types of truncated CPW grounds are particularly well suited to suppress spurious reflections and improve radiation efficiency.

Optimized parameters used in Computer Simulation Technology (CST) Microwave Studio after iterative tuning are summarized in Table 1. The elliptic radiating patch with $R = 19\,\text{mm}$ and $R1 = 14\,\text{mm}$, circular stub with $R2 = 10\,\text{mm}$. This notch triangle pressure is 12.5 mm in depth. The feedline's dimensions are $Lf = 35\,\text{mm}$ and $Wf = 3.39\,\text{mm}$, with a gap of $Gw = 0.4\,\text{mm}$ on its either side. Copper metallization thickness is 0.035 mm. The extended configuration introduces a full copper reflector for gain and directivity improvement at lower frequencies, where monopole antennas are known to lack performance. The reflector is located at an optimum gap from the substrate, and it intensifies the forward radiation by constructive interference but suppresses back-lobe radiation. It offers a low-cost, fabricable alternative in an uncomplicated way.

3. STEPWISE DESIGN EVALUATION OF ANTENNA

Figure 2 illustrates the systematic methodology, optimization, and validation of the proposed CPW-fed half-moon monopole ultra-wideband (UWB) antenna. The design process began with developing a conventional CPW-fed half-moon monopole antenna operating over the 3.1–10.6 GHz UWB frequency range. The antenna geometry was then optimized to achieve lower-frequency operation while maintaining a wide impedance bandwidth. Once the desired performance criteria

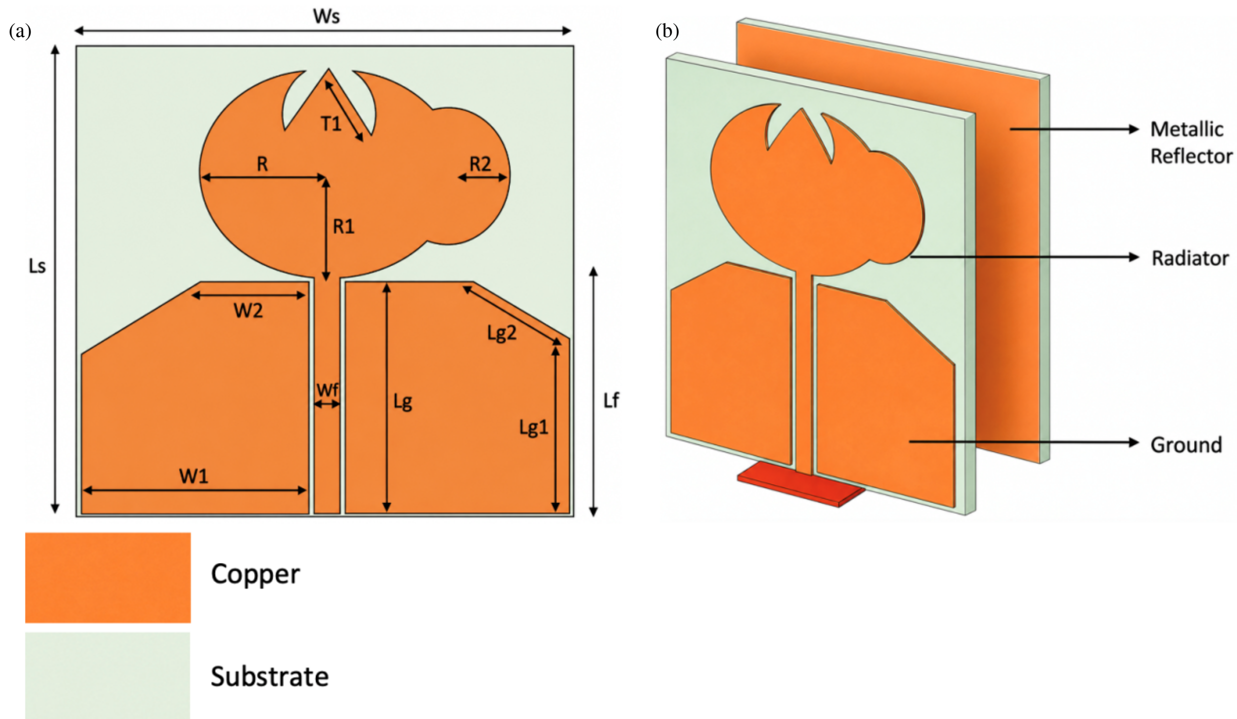

FIGURE 1. UWB antenna configuration. (a) Geometrical parameters of the proposed stub-loaded half-moon patch antenna and (b) antenna with metallic back reflector.

TABLE 1. Parameters of the proposed ultra-wideband CPW-fed half-moon monopole patch antenna.

Parameters	Values (mm)
Substrate Width (Ws)	70
Substrate Length (Ls)	70
Substrate Thickness (h)	1.6
Copper Thickness (t)	0.035
Feedline Length (Lf)	35
Feedline Width (Lw)	3.39
CPW gap between of Feedline (Gw)	0.4
CPW Length of main (Lg)	34.6
CPW Length of secondary ($Lg1$)	27
CPW width lower ($W1$)	32.905
CPW width Upper ($W2$)	16.405
CPW Narrow Length ($Lg2$)	18.166
Elliptical Cylinder Horizontal, (R)	19
Elliptical Cylinder Vertical, ($R1$)	14
Triangle Length, (Tl)	12.50
Spherical ($R2$)	10

were achieved, a full-copper metallic reflector was integrated behind the antenna to enhance its radiation characteristics.

Subsequently, the reflector's influence on antenna performance was thoroughly investigated, particularly in reflection coefficient, impedance bandwidth, gain, and radiation behavior. Several reflector configurations and spacing parameters were evaluated through an iterative optimization process until the desired performance objectives were satisfied. Finally, a comparative analysis between antennas with and without a metallic reflector was conducted to quantify improvements achieved in gain enhancement and radiation directivity. This systematic workflow ensured the development of a compact, high-gain, and wideband antenna suitable for GPR and other broadband sensing applications.

3.1. Design and Simulation of the Antenna to Attain UWB Frequency Response

In the first stage, a CPW-fed half-moon monopole patch antenna was designed using CST Microwave Studio instead of High Frequency Structure Simulator (HFSS), as compared and discussed in [29]. The design process involved careful adjustment of substrate dimensions, a ground plane configuration, and a feed line geometry to ensure broadband impedance matching and radiation stability. The antenna was simulated in the 1–11 GHz frequency range, and baseline performance parameters, including the reflection coefficient, are extracted for evaluation. The antenna development process followed a stepwise progression, as illustrated in Fig. 3. The reflection coefficient plot for the design process is shown in Fig. 3(e).

The initial elliptical patch antenna (Fig. 3(a)) provided a baseline monopole structure with multiple resonance bands within the required UWB bandwidth. $|S_{11}|$ plot depicts the resonance at 3.5 GHz (2.5–4.7 GHz), 6.9 GHz and 9 GHz (8.5–10.1 GHz). To improve impedance matching over the required bandwidth, a circular slot was etched on top of the elliptical radiator (Fig. 3(b)), which introduced additional resonant modes and covered the entire UWB spectrum except at 4.7 GHz.

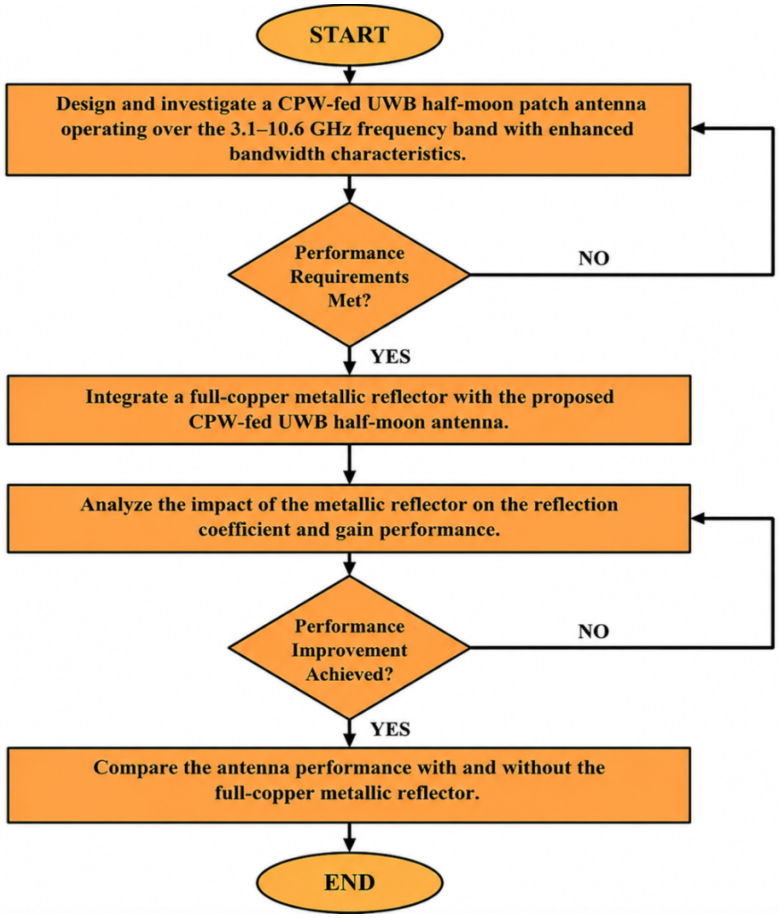

FIGURE 2. Flowchart illustrating the design, optimization, and performance evaluation procedure of the proposed CPW-fed half-moon UWB antenna with a full-copper metallic reflector.

In the third stage, the elliptical radiator was modified by integrating a triangular stub in the circular slot as in Fig. 3(c). Introducing this triangle improved capacitive coupling, leading to deeper resonances and better impedance matching across the UWB (2 GHz to 10.3 GHz). However, the bandwidth was further extended to the higher cutoff frequency, and gain enhancement was still inadequate for demanding UWB applications such as GPR and biomedical sensing. A circular stub is added on the radiator's lateral side. In the final design (Fig. 3(d)), the proposed CPW-fed half-moon monopole antenna integrates three complementary features: an elliptical section for fundamental resonance, a triangular stub for higher-frequency stabilization, and a circular stub to broaden impedance bandwidth. The hybrid geometry, combined with a CPW feed and truncated ground planes, achieves wideband operation with consistent $|S_{11}|$ below -10 dB over a 1.9 GHz–10.7 GHz range. Thus, the proposed UWB CPW-fed half-moon monopole patch antenna (Fig. 3(d)) was chosen as the final design, as it successfully addresses the limitations of the earlier configurations while maintaining a compact, fabrication-friendly structure.

The comparative performance of the reflection coefficient shows that the basic elliptical patch antenna has a partial UWB coverage with several resonant dips. When the elliptical patch is etched with a circular slot on top, additional resonances are generated, which enhance impedance matching across mid-band frequencies, although the response at higher frequencies remains inconsistent. Adding a triangular stub offers stronger resonant characteristics, with $|S_{11}|$ values exceeding -25 dB near 8.5 GHz and extended operation up to 10.7 GHz. By contrast, after adding a circular stub, the antenna achieves the widest impedance bandwidth, spanning approximately 1.00–11.0 GHz, with multiple resonances but unstable $|S_{11}|$ values lying near -10 dB throughout the band.

3.2. Integration of the Full Copper Reflector

The second stage introduced a full-copper reflector with 0.035 mm thickness behind the radiating patch at a distance of 35 mm (as in Fig. 1(c)). For gain optimization, the distance and separation between the antenna and reflector were varied systematically, where all models we simulated were under the same electromagnetic conditions to make a fair comparison. These analyses allow quantifying effects of the reflector on constructive interference, back-lobe suppression, and beam directionality. To enhance radiation performance, a passive full-copper reflector was used ($140 \times 140\,\text{mm}^2$), which redirects backward-propagating energy into the forward direction. Taking advantage of this allows gain and directivity to be improved while keeping the design simple, low-cost,

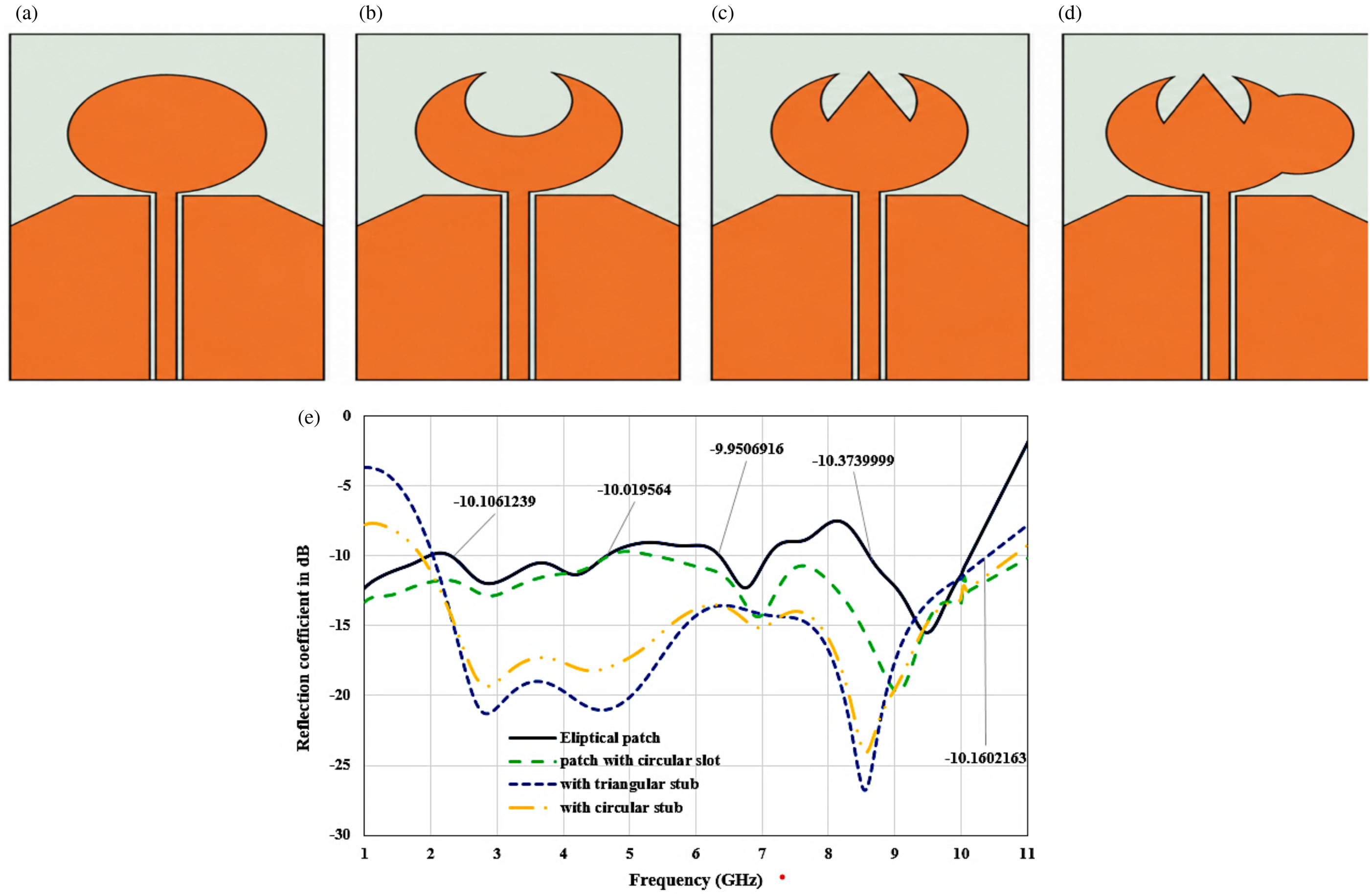

FIGURE 3. Evolution of antenna geometries and corresponding Reflection Coefficient plot: (a) Elliptical patch with truncated ground, (b) half-moon patch antenna, (c) triangular stub loaded patch antenna, (d) circular stub-loaded antenna (proposed structure), and (e) reflection coefficient plot.

and requiring neither active components nor complicated multilayered structures.

3.3. Validation and Comparative Analysis of Antenna with and without Reflector

In the final stage, simulation results from the standalone and reflector-assisted antennas were compared. Performance improvements were validated when the reflector-integrated design demonstrated enhanced gain and directivity while maintaining acceptable impedance bandwidth and reflection coefficient. Fig. 4 depicts the effect of the reflector plate on the reflection coefficient and antenna gain. After adding the reflector plate, the antenna resonance shifts towards the lower cutoff frequency at 2 GHz, and the bandwidth ranges from 2.2 GHz to 10.6 GHz, which is satisfactory for UWB operations. Gain has significant improvement and remains above 6.5 dBi over the entire bandwidth with the reflector. At 3 GHz gain raised from 5.5 dBi to 6.6 dBi and at 8 GHz gain raised from 6.4 dBi to 7.7 dBi. The simulated results were then justified with measured results, which are aligned with the study's objectives.

Figure 4(b) illustrates the radiation efficiency of the proposed antenna with and without the metallic reflector. The antenna exhibits high efficiency across the entire operating band, exceeding 84% in both cases. Including the metallic reflector provides a moderate improvement of approximately 3–4%, resulting in a peak efficiency of about 96% near 7 GHz. This enhancement is attributed to improved forward radiation and reduced power loss due to back radiation suppression. The results confirm that the reflector improves the radiation performance while maintaining stable efficiency over the UWB operating band. Fig. 4(c) shows the effect of the reflector spacing on the antenna reflection coefficient. At the lowest gap of 5 mm, the antenna impedance degrades significantly, and the curve shifts above -10 dB. As the gap is increased above 35 mm, the reflector effect is negligible. Thus, best impedance matching at a reflector distance of 35 mm, with the lowest $|S_{11}|$ values and widest operating bandwidth, is selected.

4. MEASURED RESULT ANALYSIS

This section presents simulated and experimental performance of the proposed CPW-fed half-moon and elliptical UWB antenna configurations. It covers the analysis of the reflection coefficient, the spacing effect of the metallic reflector, and the radiation characteristics. Numerical simulations are carried out in CST Microwave Studio, followed by experimental validation in antenna fabrication and measurement taken with a Vec-

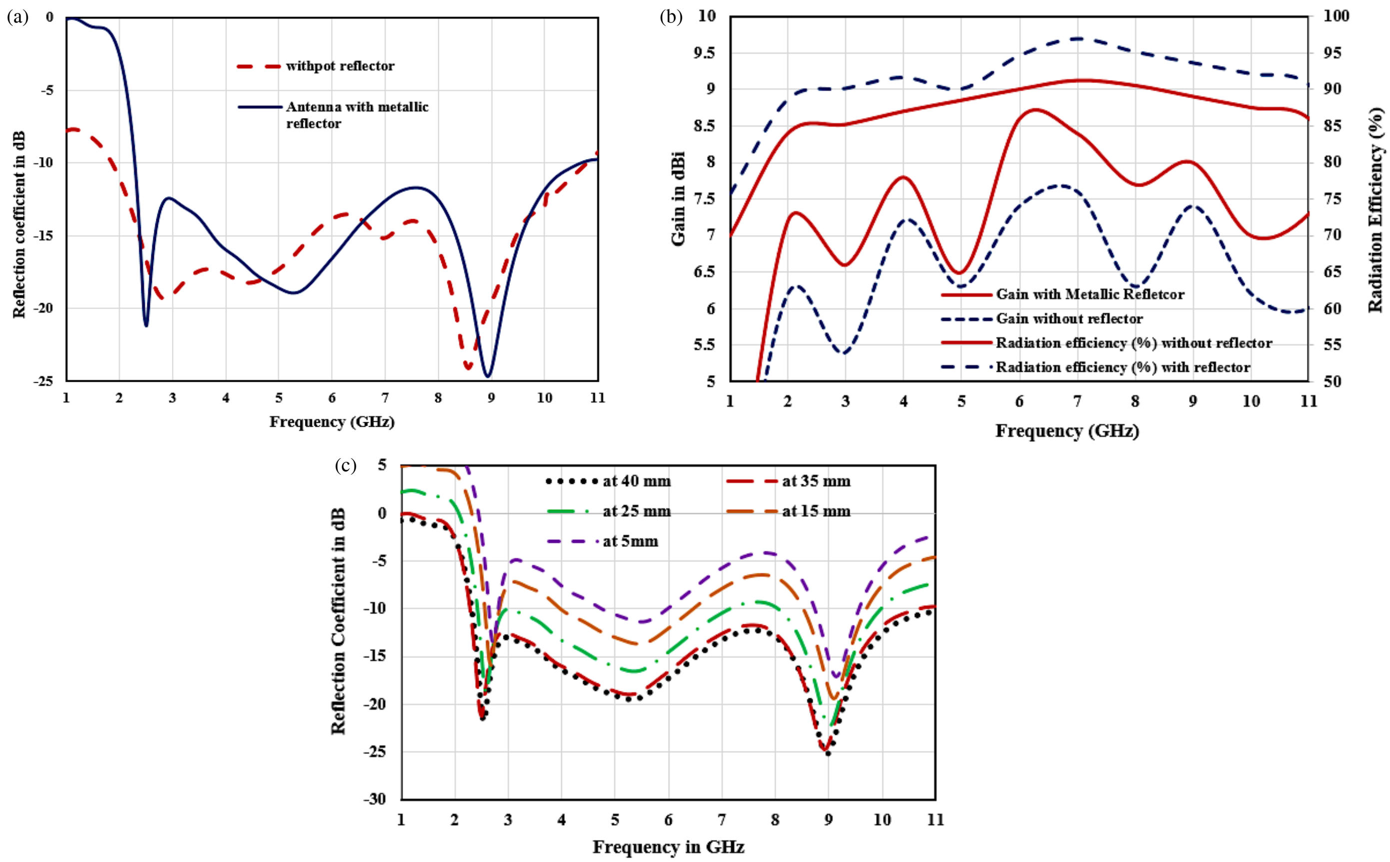

FIGURE 4. Antenna performance with and without metallic reflector, (a) reflection coefficient plot, (b) gain and efficiency, and (c) parametric analysis of metallic reflector spacing on reflection coefficient.

tor Network Analyzer (VNA). The analysis starts from an S_{11} comparison between simulated and measured values in terms of impedance matching and bandwidth behaviour. The effect of the 35 mm reflector gap on reflection coefficient and antenna performance is investigated, followed by an assessment of radiation-field distributions at various frequencies. Collectively, these results validate the simulation model and demonstrate practical suitability of the proposed antenna design for broadband and ground-penetrating radar (GPR) applications. Antenna measurement results are depicted in Fig. 5, which shows the reflection coefficient and screenshots of the measurement setup.

The measured results show a similar overall trend, although S_{11} values are slightly higher, which is commonly attributed to fabrication tolerances, connector losses, and variations in experimental environment. Despite these practical deviations, the measured S_{11} remains below -10 dB at key frequencies, including around 2 GHz and 10.8 GHz, confirming effective performance within the UWB range. The close alignment between predicted and tested responses verifies the accuracy of the modelled design and confirms that adding a full copper reflector maintains the antenna's impedance characteristics. Fabrication tolerances, such as variations in patch dimensions, feed width, substrate properties, and reflector spacing, can influence the antenna's resonant frequencies, impedance bandwidth, and gain. However, owing to its ultra-wideband operation, the proposed antenna exhibits reasonable robustness against small manufacturing deviations, maintaining satisfactory performance for GPR applications.

Figure 6(a) shows the antenna's measured gain over the operating bandwidth. The measured and simulated patterns are in good agreement, indicating that the proposed antenna can effectively communicate with external devices in sensing applications. The results show that the antenna's gain variation is stable in the range of about 5.5 dBi to 8.7 dBi in the operating band to ensure consistent radiation in UWB systems. The appearance of numerous gain peaks at various frequencies indicates that there are multiple resonances, and such a behavior is typical of UWB antennas. Such resonances help preserve relatively uniform gain in the entire band. Additionally, the comparison between two variants, with and without a metallic reflector, suggests that using the reflector increases antenna gain significantly. This can be mainly explained by reducing the backward radiation from the antenna and its increase directed forward. In other words, there is an increase in directivity. The reason behind such gain enhancement is based on reflector theory in which constructive interference takes place.

The 2-D radiation pattern of the proposed antenna at different frequencies is also examined in Figs. 6(b)–(d). For both conditions, with and without a metallic reflector, at 4.5 GHz and 7 GHz, the antenna has an omnidirectional radiator in the E-plane and bidirectional radiation patterns in the H-plane. This

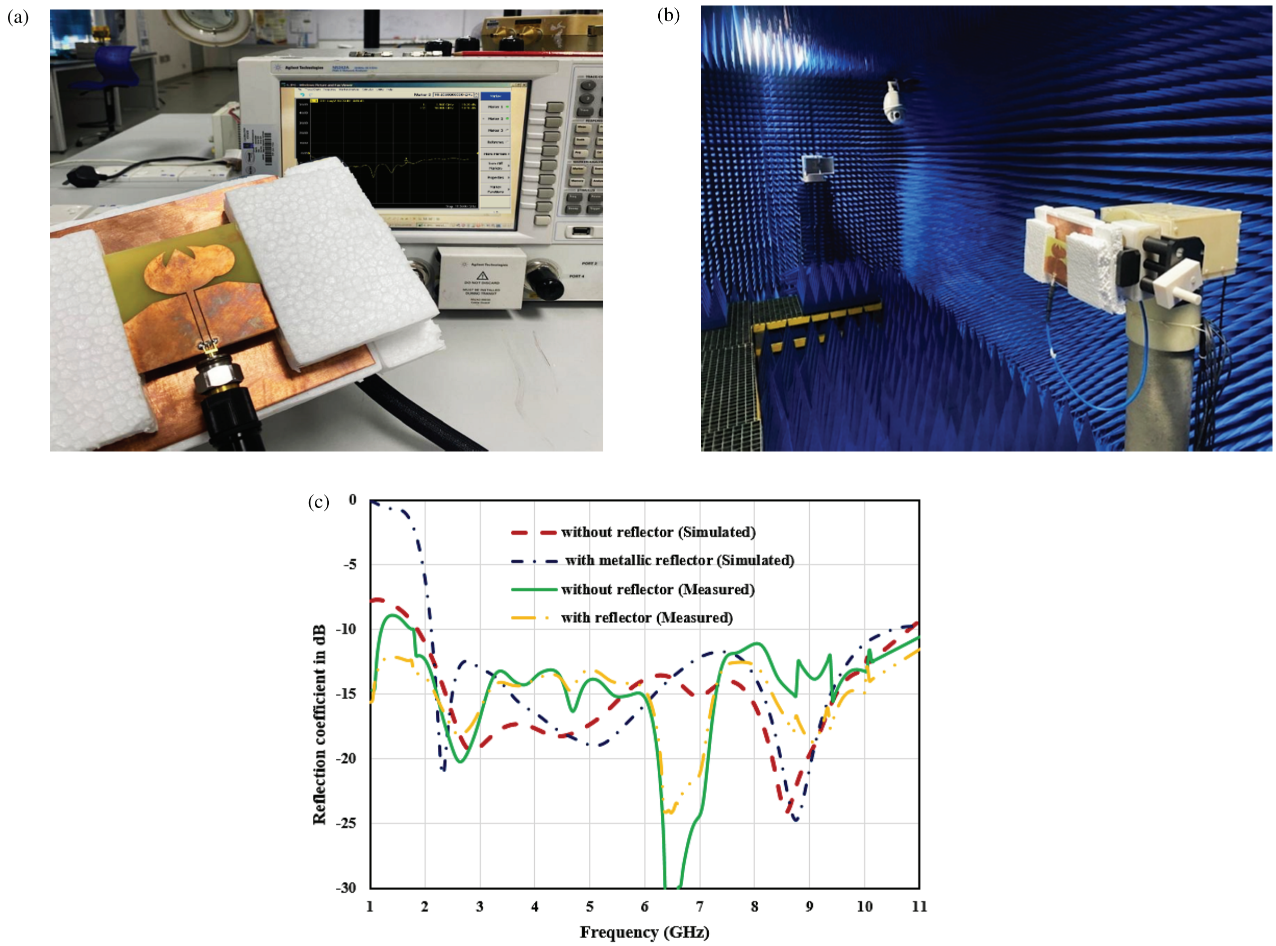

FIGURE 5. (a) and (b) Screenshots for measurement setup of antenna with VNA and in an anechoic chamber, and (c) measured reflection coefficient of antenna with and without reflector plate.

is a characteristic feature of the monopole-type ultra-wideband antenna. As a result, the antenna becomes a uniform radiator along the azimuth plane, hence making the antenna suitable for sensing applications where uniformity is expected. At 8.5 GHz, the small distortions in the radiation patterns may be due to the occurrence of higher-order modes of excitation on the antenna's radiating surface. Additionally, including a metallic reflector results in an improvement in the directivity pattern by reducing backward radiation components and thus focusing the radiation in one direction, as clearly indicated by the increased strength of the major lobe. The appearance of side lobes and nulls at some angles is attributed to the constructive and destructive interference of waves emitted by different regions of the antenna. Generally, steady and reproducible radiation patterns at different frequencies indicate that the antenna is a reliable source of radiation. Furthermore, to justify the antenna's radiation and gain results, 3-D radiation plots are also plotted for both with and without a metallic reflector in Fig. 7. At all frequencies, gain improvement is attained with the reflector plate.

From a structural perspective, many gain-enhanced antennas reported in the literature rely on frequency-selective surfaces (FSSs), metamaterials, artificial electromagnetic materials, or array configurations to improve radiation performance. Although these approaches can provide significant gain enhancement, they often increase fabrication complexity, design cost, and overall system size. In contrast, the proposed antenna avoids such complexities by employing a compact half-moon monopole radiator integrated with a metallic reflector, resulting in a simple, low-cost, easy-to-fabricate structure suitable for practical deployment. As presented in Table 2, the proposed antenna is compared with recently reported studies [30–39], demonstrating its competitive performance in bandwidth, gain, compactness, and implementation simplicity.

The comparison also indicates that several recent studies, such as Gupta et al. [30], Patil et al. [31], and Shen et al. [32], primarily focus on microwave imaging algorithms, breast phantom characterization, or GPR system implementation rather than antenna design optimization. Consequently, direct comparisons of gain and bandwidth are not always available. Nevertheless, these studies highlight the growing importance of compact and efficient UWB antennas for imaging and sensing applications.

Overall, the proposed antenna offers an attractive balance among wide bandwidth, moderate-to-high gain, compact size, low complexity, and fabrication simplicity. While some advanced Vivaldi and array-based antennas achieve higher gains,

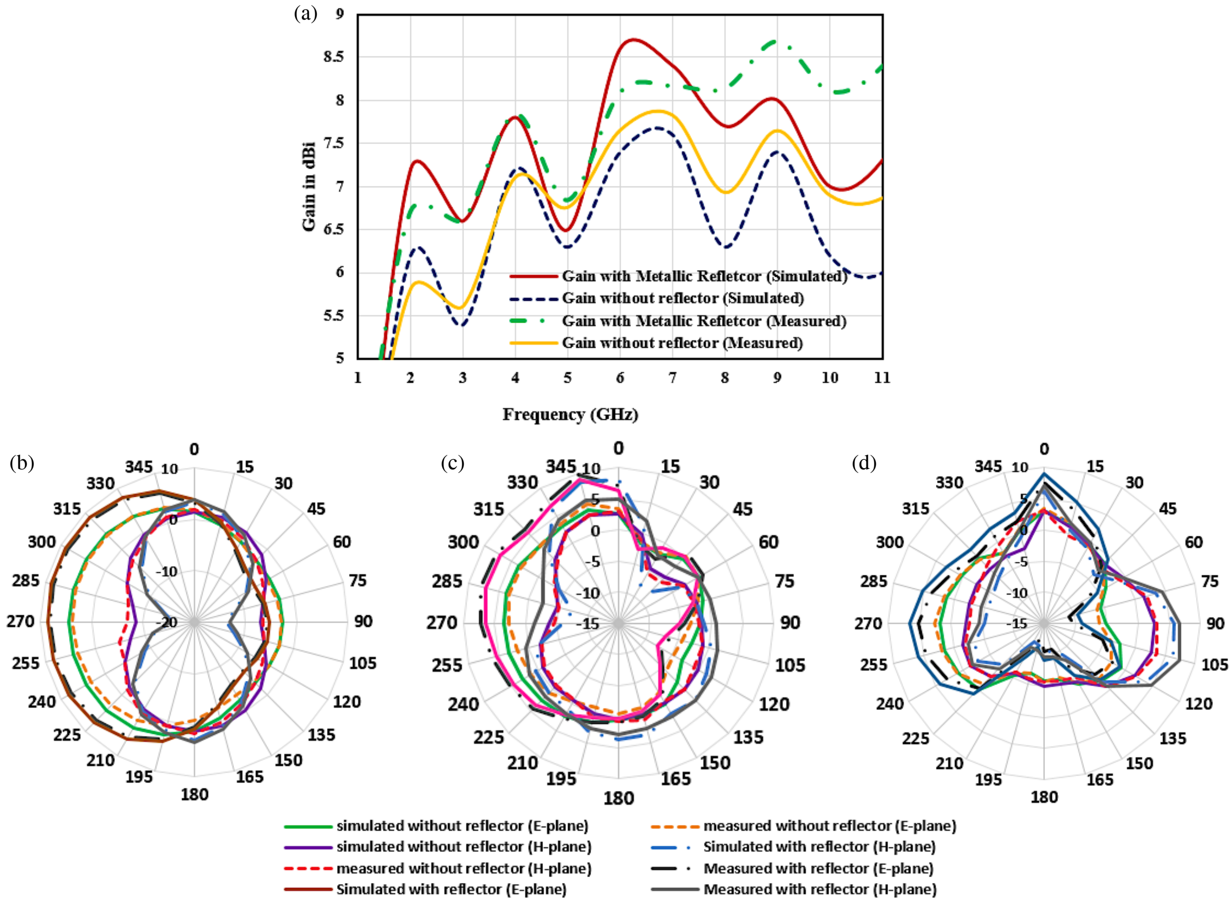

FIGURE 6. Radiation performance, (a) gain, (b) radiation pattern at 4.5 GHz, (c) at 7 GHz, and (d) 8.5 GHz.

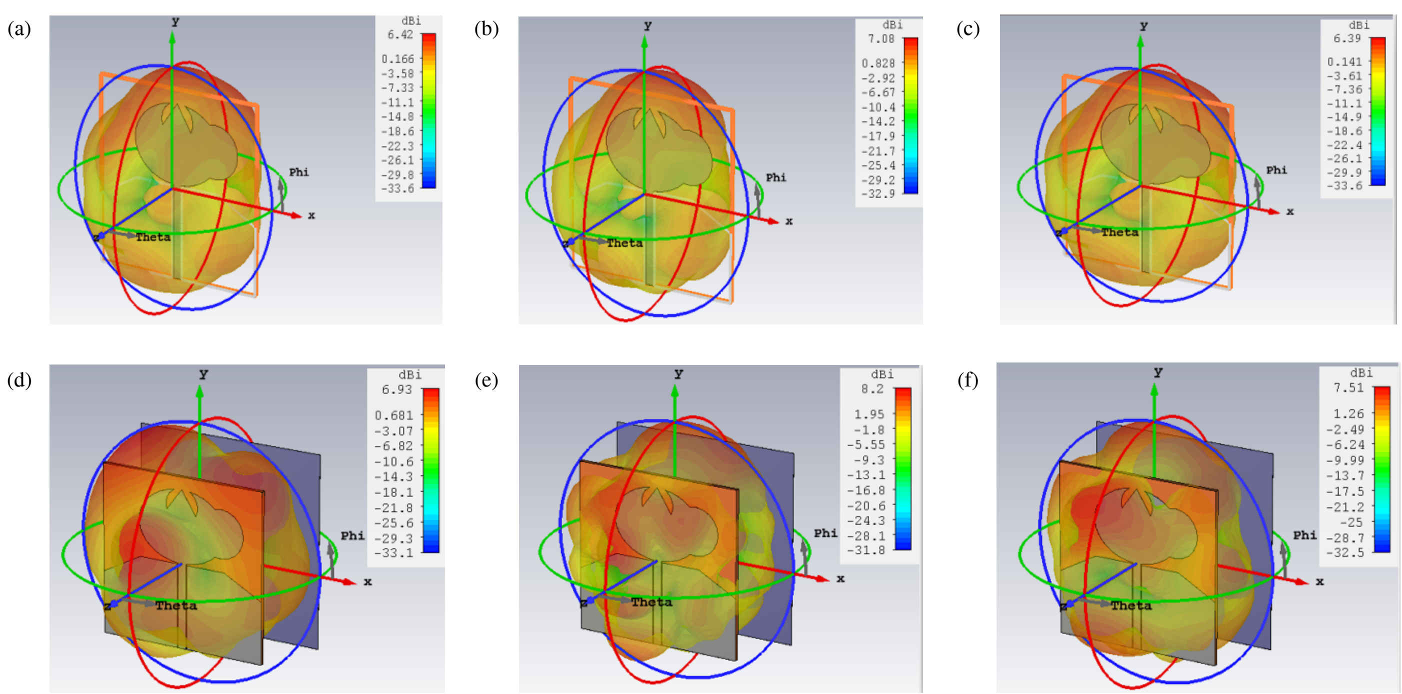

FIGURE 7. 3-D radiation pattern of antenna (a)–(c) without reflector GHz, (d)–(f) with reflector, (a) and (d) at 4.5 GHz, (b) and (e) at 7.5 GHz, (c) and (f) at 9.5 GHz.

TABLE 2. Summary of antenna with existing antenna designed for UWB sensing and GPR applications.

Ref.	Antenna Type	Frequency Range (GHz)	Bandwidth (%)	Peak Gain (dBi)	Size (mm^3)	Reflector/ Metasurface	Application
[30]	Dielectric Resonator Antenna (DRA)	UWB	NR	NR	NR	No	Breast Tumor Localization/ Microwave Imaging
[31]	UWB Sensing Antenna	UWB	NR	NR	NR	No	Breast Phantom Characterization
[32]	Aperture-Slot Antipodal Vivaldi Antenna	0.5–3.0*	$> 140^*$	8.3	$40 \times 40 \times 1.6$	FSS Reflector	UWB/GPR
[33]	VNA-Based GPR System	NR	NR	NR	NR	No	GPR
[34]	Modified Straight-Tapered Vivaldi Antenna	0.8–4.0*	$> 130^*$	9–11*	Compact	No	GPR
[35]	Semicircular UWB Monopole	3–11	114	8.3	$40 \times 40 \times 1.6$	FSS Reflector	Breast Tumor Localization/ Microwave Imaging
[36]	Directional Bow-Tie Antenna	0.317–0.94	98.6	9.3	$0.38\lambda \times 0.38\lambda \times 0.05\lambda$	Metallic Reflector + Metamaterial	GPR
[37]	Dual-Polarized Vivaldi Array	0.9–4.0	126	15.2	Compact Array	Artificial Electromagnetic Material	GPR
[38]	CPW-Fed UWB Monopole	3.1–10.6	109	14.8	$80 \times 80 \times 1.6$	Metallic Reflectors	UWB Radar
[39]	Planar UWB Antenna	0.79–2.99	116	6.5	$120 \times 120 \times 1.6$	No	SFCW-GPR
This work	**Half-Moon Monopole with Metallic Reflector**	**2–10.8**	**137.5%**	**8.7**	**70×70**	**Metallic Reflector**	**GPR**

the proposed design provides a practical and cost-effective alternative for GPR applications without requiring sophisticated electromagnetic structures or large antenna arrays. This combination of performance and simplicity makes the proposed antenna a promising candidate for portable and real-world GPR systems.

Table 2 presents a comparison between the proposed half-moon monopole antenna and several recently reported UWB antennas and GPR-related systems. The comparison highlights key performance parameters, including operating frequency range, bandwidth, gain, antenna size, gain-enhancement techniques, and intended applications. Among reviewed antennas, the proposed design achieves a wide operating bandwidth of 2–10.8 GHz, corresponding to a fractional bandwidth of 137.5%, which is higher than that of several reported monopole-based antennas, including a semicircular UWB monopole by Din et al. [35] (114%), a CPW-fed monopole reported in [38] (109%), and a planar UWB antenna reported in [39] (116%). This wide bandwidth enables the proposed antenna to support high-resolution GPR imaging and target detection over a broad frequency spectrum.

In terms of gain performance, the proposed antenna provides a peak gain of 8.7 dBi, which is comparable to the FSS-backed semicircular monopole reported by Din et al. [35] (8.3 dBi) and the directional bow-tie antenna reported by Pi et al. [36] (9.3 dBi). Although higher gains have been achieved by Vivaldi-based antennas and antenna arrays, such as the dual-polarized Vivaldi array reported by Hu et al. [37] (15.2 dBi) and the reflector-backed monopole reported by Turkmen-Kucuksari et al. [38] (14.8 dBi), these designs generally require larger apertures, more complex structures, array configurations, or artificial electromagnetic materials. In contrast, the proposed antenna achieves competitive gain using only a simple metallic reflector.

In real-world GPR applications, antenna performance may be affected by soil moisture variations, ground inhomogeneity, surface roughness, and clutter, which can cause signal attenuation and distortion. Additionally, maintaining a constant antenna-to-ground distance and minimizing electromagnetic interference are practical challenges during field measurements. Despite these factors, the proposed reflector-backed half-moon monopole antenna offers a wide bandwidth, directional radiation, and compact size, making it well suited for GPR deployment in diverse environments. Future work will focus on validating the proposed antenna under real-world GPR conditions, including different soil types, moisture levels, and buried target scenarios. Further investigations may also explore antenna arrays, advanced reflector/metasurface designs, and machine learning-based signal processing techniques to enhance detection accuracy, penetration depth, and imaging performance in practical GPR applications.

5. CONCLUSION

This paper has presented a CPW-fed half-moon monopole ultra-wideband (UWB) antenna integrated with a full-copper reflector and demonstrated its design, simulation, fabrication, and experimental validation for ground-penetrating radar (GPR) applications. By employing a reflector spacing of 35 mm, the proposed antenna achieved an extended operating bandwidth of 2–10.8 GHz, along with a stable gain ranging from 6.5 dBi to 8.7 dBi in UWB. Incorporating a metallic reflector significantly improved the antenna's radiation characteristics by suppressing back-lobe radiation and directing more energy toward the forward direction, which is essential for enhancing subsurface penetration and imaging resolution in GPR systems. Furthermore, excellent agreement between the simulated and measured results validates the effectiveness and reliability of the proposed design. The achieved performance demonstrates that a simple reflector-based approach can provide high gain and wideband operation without the need for complex, expensive, or artificial electromagnetic structures. Owing to its compactness, low cost, ease of fabrication, and favorable radiation characteristics, the proposed antenna represents a promising candidate for practical GPR systems and other broadband sensing applications.

ACKNOWLEDGEMENT

The authors express their sincere gratitude to Universiti Teknikal Malaysia Melaka (UTeM), the Ministry of Higher Education (MOHE), Asia Pacific University (APU), and the Strategic Research Institute (SRI) for their support of this project.

REFERENCES

[1] Alnaiemy, Y., M. Q. Abdalrazak, Z. Salam, and T. A. Elwi, "on the performance of CRLH antenna loaded with AMC reflector for direct antenna modulation process," *Progress In Electromagnetics Research C*, Vol. 166, 244–256, 2026.

[2] Al-Gburi, A. J. A., I. B. M. Ibrahim, Z. Zakaria, and N. F. B. M. Nazli, "Wideband microstrip patch antenna for sub 6 GHz and 5G applications," *Przegląd Elektrotechniczny*, Vol. 97, No. 11, 26–29, 2021.

[3] Al-Gburi, A. J. A., I. M. Ibrahim, Z. Zakaria, M. K. Abdulhameed, and T. Saeidi, "Enhancing gain for UWB antennas using FSS: A systematic review," *Mathematics*, Vol. 9, No. 24, 3301, Dec. 2021.

[4] Mohanna, M. M., E. Abdallah, H. El-Hennawy, and M. A. Attia, "A novel high directive willis-sinha tapered slot antenna for GPR application in detecting landmine," *Progress In Electromagnetics Research C*, Vol. 80, 181–198, 2018.

[5] Al-Gburi, A. J. A., Z. Zakaria, I. M. Ibrahim, and E. B. A. Halim, "Microstrip patch antenna arrays design for 5G wireless backhaul application at 3.5 GHz," in *Recent Advances in Electrical and Electronic Engineering and Computer Science*, 77–88, Springer, Singapore, 2022.

[6] Ali, A., J. Tong, J. Iqbal, U. Illahi, A. Rauf, S. U. Rehman, H. Ali, M. M. Qadir, M. A. Khan, and R. M. Ghoniem, "Mutual coupling reduction through defected ground structure in circularly polarized, dielectric resonator-based MIMO antennas for sub-6 GHz 5G applications," *Micromachines*, Vol. 13, No. 7, 1082, Jul. 2022.

[7] Al-Gburi, A. J. A., "Do we really need frequency-selective surface and metasurface reflectors for antenna gain enhancement, or are metallic reflectors enough?" *International Journal of Antennas and Propagation*, Vol. 2026, No. 1, 2141943, 2026.

[8] Mohammed, D. Z. and A. J. A. Al-Gburi, "Compact, gain-enhanced 5G mmWave antenna with metallic ground-backed reflector for high-speed railway communication systems," *High-speed Railway*, Vol. 3, No. 4, 281–292, 2025.

[9] Zidan, M., M. Islam, N. Misran, and A. Abdullah, "Conductive ground reflector-enabled patch antenna for high-gain 5G sub-6 GHz and multiband systems," *Proceedings of The Bulgarian Academy of Sciences*, Vol. 78, No. 12, 1879–1885, 2025.

[10] Jayamani, K., V. Vinodhini, V. Gomathi, S. Vanaja, S. Kalaivani, and V. Chinnammal, "A novel UWB microstrip patch antenna des for cardio activity monitoring application," *Materials Today: Proceedings*, Vol. 47, 340–344, 2021.

[11] Kalita, A. J., N. Barkataki, and U. Sarma, "Design and optimisation of inverted U-shaped patch antenna for ultra-wideband ground-penetrating radar applications," *Engineering Proceedings*, Vol. 87, No. 1, 25, Mar. 2025.

[12] Kumari, T., A. Senapati, and A. N. Ghazali, "A UWB-specific metasurface-inspired MIMO antenna with enhanced isolation and gain," in *Proceedings of the 1st International Conference on Cognitive & Cloud Computing (IC3Com 2024)*, 30–36, 2025.

[13] Kundu, S., "Gain augmentation of a triple notched ultra-wideband antenna using compact uniplanar frequency selective surface for ground penetrating radar," *IETE Journal of Research*, Vol. 69, No. 2, 813–824, 2023.

[14] Luadang, B., C. Ainthachot, P. Janpangngern, K. Pookkapund, D. Torrungrueng, M. Krairiksh, and C. Phongcharoenpanich, "EBG-backed ultrawideband circularly polarized Archimedean spiral antenna scheme for IoT applications," *Scientific Reports*, Vol. 15, No. 1, 11769, 2025.

[15] Raza, A., W. Lin, M. K. Ishfaq, M. Inam, F. Masud, and M. H. Dahri, "A wideband reflector-backed antenna for applications in GPR," *International Journal of Antennas and Propagation*, Vol. 2021, No. 1, 3531019, 2021.

[16] Saeidi, T., A. R. H. Alhawari, A. H. M. Almawgani, T. Alsuwian, M. A. Imran, and Q. Abbasi, "High gain compact UWB antenna for ground penetrating radar detection and soil inspection," *Sensors*, Vol. 22, No. 14, 5183, Jul. 2022.

[17] Gupta, A., P. Chawla, A. Kansal, and K. Singh, "An active and low-cost microwave imaging system for detection of breast cancer using back scattered signal," *Current Medical Imaging*,

Vol. 18, No. 5, 460–475, 2022.

[18] ALtalqi, F., H. Mabchour, and A. Echchelh, "Design of a high efficiency monopole antenna array for GPR application," *Journal of Nano- and Electronic Physics*, Vol. 16, No. 2, 02015, 2024.

[19] An, W., X. Tian, J. Wang, and S. Wang, "Low-profile dual-polarized double-layer microstrip antenna for 5G and 5G Wi-Fi," *Micromachines*, Vol. 14, No. 5, 942, 2023.

[20] Awan, D., S. Bashir, S. Khan, S. S. Al-Bawri, and M. Dalarsson, "Uwb antenna with enhanced directivity for applications in microwave medical imaging," *Sensors*, Vol. 24, No. 4, 1315, 2024.

[21] Hussain, M., M. A. Sufian, M. S. Alzaidi, S. I. Naqvi, N. Hussain, D. H. Elkamchouchi, M. F. A. Sree, and S. Y. A. Fatah, "Bandwidth and gain enhancement of a CPW antenna using frequency selective surface for UWB applications," *Micromachines*, Vol. 14, No. 3, 591, 2023.

[22] Janarthanan, S., M. A. Bennet, K. Jayaram, and V. Govindaraj, "Compact dual-band microstrip patch antenna design for 5G wireless networks using grey wolf optimization," *Tehnički Vjesnik*, Vol. 32, No. 4, 1330–1335, 2025.

[23] Rizvi, S. N. R., W. A. Awan, and N. Hussain, "Design and characterization of miniaturized printed antenna for UWB communication systems," *Journal of Electrical Engineering & Technology*, Vol. 16, No. 2, 1003–1010, 2021.

[24] Sen, G. and S. Das, "Interdigital coupled compact FSS reflector for UWB antenna gain enhancement," *Progress In Electromagnetics Research Letters*, Vol. 120, 47–52, 2024.

[25] Tariq, S., W. T. Sethi, A. A. Rahim, F. Faisal, and T. Djerafi, "A metasurface assisted pin loaded antenna for high gain millimeter wave systems," *Scientific Reports*, Vol. 15, No. 1, 12056, 2025.

[26] Van Verre, W., F. J. W. Podd, X. Gao, L. A. Marsh, J. L. Davidson, D. J. Daniels, and A. J. Peyton, "Reducing the induction footprint of ultra-wideband antennas for ground-penetrating radar in dual-modality detectors," *IEEE Transactions on Antennas and Propagation*, Vol. 69, No. 3, 1293–1301, Mar. 2021.

[27] Xu, H., J. Yan, G. Feng, Z. Jia, and P. Jing, "Rock layer classification and identification in ground-penetrating radar via machine learning," *Remote Sensing*, Vol. 16, No. 8, 1310, Apr. 2024.

[28] Zheng, W., T. Hao, X. Li, and W. Luo, "Experimental validation of the horizontal resolution improvement by ultra-wideband metasurfaces for GPR systems," *NDT & E International*, Vol. 147, 103179, Oct. 2024.

[29] Al-Gburi, A. J. A., "CST vs HFSS: A comparative analysis for antenna and microwave engineering," *International Journal of Antennas and Propagation*, 2 733 569, 17 pages, 2026.

[30] Gupta, A., S. K. Yadav, C. A. D. Durai, V. Kuamr, M. H. Alsharif, P. Uthansakul, and M. Uthansakul, "Enhanced breast tumor localization with DRA antenna backscattering and GPR algorithm in microwave imaging," *Results in Engineering*, Vol. 24, 103044, 2024.

[31] Patil, S., K. Singh, and A. Naik, "Examination of breast phantom layers using UWB antenna sensing technique," *International Journal of Electrical and Computer Engineering Systems*, Vol. 17, No. 4, 307–315, 2026.

[32] Shen, F., N. Yang, C. Xia, T. Wan, and J. Kang, "A compact aperture-slot antipodal Vivaldi antenna for GPR systems," *Sensors*, Vol. 26, No. 3, 810, 2026.

[33] Prasanth, A., P. Abhinav, A. Ramachandran, A. Kanakaraj, K. Sajith, and K. K. Ajith, "Experimental ground penetrating radar using vector network analyzer," in *2024 IEEE Space, Aerospace and Defence Conference (SPACE)*, 15–18, Bangalore, India, 2024.

[34] Abbas, M. K., A. J. Salim, R. T. Hammed, and A. Sali, "Design and optimization of a modified straight-tapered Vivaldi antenna using ANN for GPR system," *Open Engineering*, Vol. 15, No. 1, 20250143, 2025.

[35] Din, I. U., S. Ullah, S. I. Naqvi, R. Ullah, S. Ullah, E. M. Ali, and M. Alibakhshikenari, "Improvement in the gain of UWB antenna for GPR applications by using frequency-selective surface," *International Journal of Antennas and Propagation*, Vol. 2022, No. 1, 2002552, 2022.

[36] Pi, S., T. Wang, and J. Lin, "Directional and high-gain ultra-wideband bow-tie antenna for ground-penetrating radar applications," *Remote Sensing*, Vol. 15, No. 14, 3522, 2023.

[37] Hu, R., F. Zhang, S. Ye, and G. Fang, "Ultra-wideband and high-gain vivaldi antenna with artificial electromagnetic materials," *Micromachines*, Vol. 14, No. 7, 1329, 2023.

[38] Turkmen-Kucuksari, O., A. Kocakaya, G. Çakır, and S. Çimen, "Gain enhancement of co-planar waveguide fed ultra-wide bandwidth monopole antenna with enlarged ground plane and metal reflectors," *AEU — International Journal of Electronics and Communications*, Vol. 126, 153422, 2020.

[39] Wu, Y., F. Shen, Y. Yuan, and D. Xu, "An improved modified universal ultra-wideband antenna designed for step frequency continuous wave ground penetrating radar system," *Sensors*, Vol. 19, No. 5, 1045, 2019.